

Figure 5. EP4 signaling decreased lysyl oxidase (LOX) protein via the c-Src-PLC γ pathway in ductus arteriosus smooth muscle cells (DASMCs). **A**, LOX protein expression in DASMCs treated with nonselective (Br-cAMP, 50 μ mol/L), protein kinase A (PKA)-selective (Brnz-cAMP, 50 μ mol/L) or Epac-selective (Me-cAMP, 50 μ mol/L) cAMP analogs for 24 h. The AE1-329 was administered in the presence or absence of the PKA inhibitor PKI (10 μ mol/L). **B**, Quantification of **A**. n=4–6, *P<0.05, **P<0.01 vs CTRL. cAMP signaling did not affect the EP4-mediated reduction of LOX protein. **C**, LOX protein expression in DASMCs treated with gallein (G β γ inhibitor, 10 μ mol/L), U73122 (PLC inhibitor, 10 μ mol/L), bis (bisindolylmaleimide: PKC inhibitor, 10 μ mol/L), or LY294002 (PI3K inhibitor, 1 μ mol/L) in the presence of AE1-329. **D**, Quantification of **C**. n=4–6, *P<0.05, **P<0.01 vs CTRL. Inhibition of PLC eliminated the EP4-mediated reduction of LOX protein. **E**, Dose-dependent effect of U73122 in DASMCs treated with AE1-329. **F**, Dose-dependent inhibitory effect of m-3M3FBS on LOX protein expression. **G** and **H**, Phosphorylation of PLC γ in DASMCs treated with PP2 (Src inhibitor) or AE1-329. **I**, Quantification of **H**. n=4–6, *P<0.05. Inhibition of Src attenuated the EP4-mediated phosphorylation of PLC γ . **J**, PP2 attenuated the EP4-mediated reduction of LOX protein. **K**, Quantification of **J**. n=4–6. *P<0.05. Whole cell lysate was used for LOX detection. AE1-329 was used at 1 μ mol/L.

through exchange protein activated by the cAMP.²² Additional downstream signaling pathways of EP4 have been demonstrated in other cell types. EP4 uses G α i and phosphoinositide 3-kinase, which are generally activated by G β γ .³⁶ In addition to these well-known signaling pathways of EP4, our findings revealed c-Src-PLC γ signaling as a novel EP4 downstream pathway, as well as the inhibitory role played by EP4 signaling in elastogenesis. This EP4-signaling pathway was found to be independent of cAMP signaling, including protein kinase A and exchange protein activated by the cAMP, and G β γ and phosphoinositide 3-kinase. Studies using colorectal and lung cancer cells have suggested that β -arrestin1 bound to EP4 activates c-Src.^{31,32} In the DA, however, we did not identify an association between EP4-c-Src signaling and β -arrestin1 using β -arrestin1-targeted siRNA (data not shown). Ma et al³⁷ clearly demonstrated that G α s and G α i proteins directly

stimulate the kinase activity of c-Src. Because the EP4 receptor is coupled to G α s and G α i, direct association between these G proteins and c-Src may activate its downstream signaling in EP4-mediated degradation of LOX protein. This possibility should be validated in a future study.

LOX is a copper-dependent amine oxidase that catalyzes the cross-linking of elastin and collagen and ensures the stability of the extracellular matrix.³⁸ Because LOX is the isoform responsible for 80% of the LOX activity in aortic SMCs,³⁹ it is essential to the maintenance of the tensile and elastic features of the vascular system.³⁸ LOX is synthesized as a pre-protein. After signal peptide hydrolysis, enzyme glycosylation, copper incorporation, and lysine tyrosylquinone generation, the enzyme is released into the extracellular space. Then, BMP-1 processes LOX, yielding the mature LOX form and its propeptide.²⁷ The mechanisms of the transcriptional regulation of

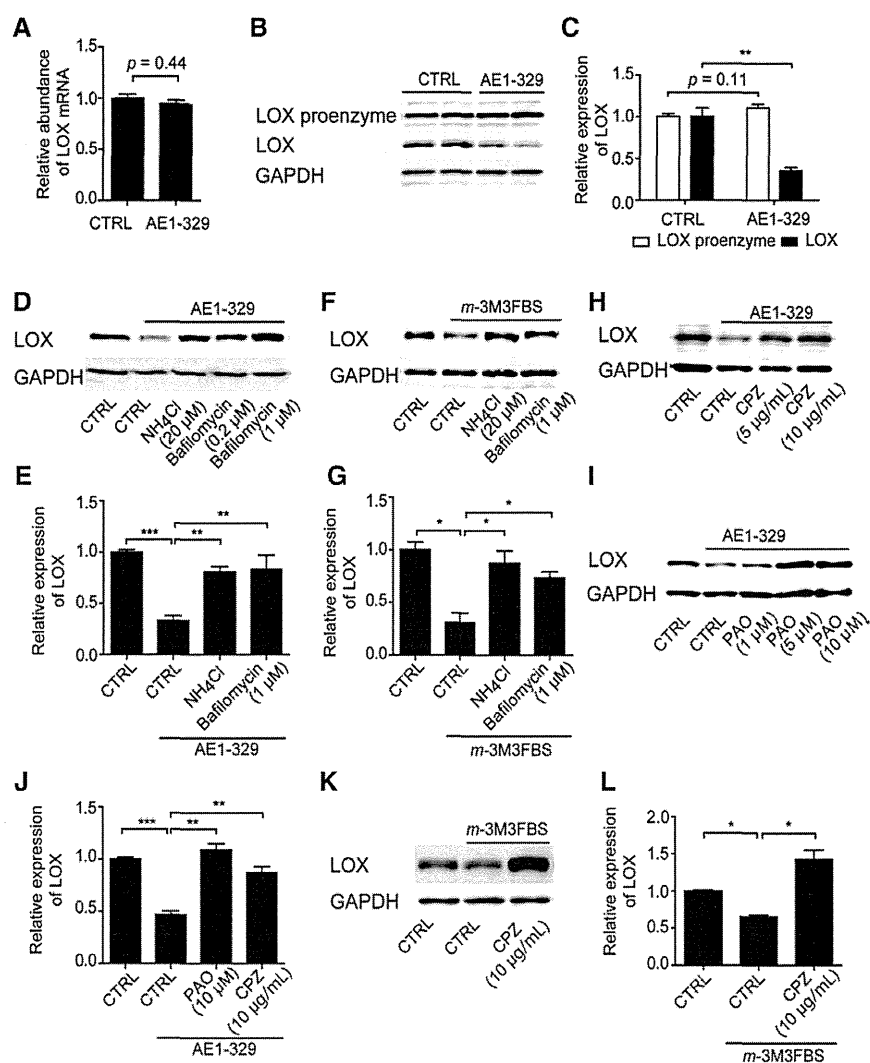


Figure 6. EP4 signaling decreased lysyl oxidase (LOX) protein through lysosomal degradation. **A** and **B**, Expression of LOX mRNA, pro-LOX, and LOX protein in ductus arteriosus smooth muscle cells (DASMCs) treated with AE1-329. mRNA of LOX and pro-LOX protein were not decreased by EP4 agonist in DASMCs. **C**, Quantification of **B**. $n=4$. **D** and **F**, Administration of lysosomal inhibitors (NH₄Cl or bafilomycin) for 24 h restored the AE1-329- or *m*-3M3FBS (0.5 μmol/L)-induced reduction of LOX protein. **E** and **G**, Quantification of **D** and **F**, respectively. $n=6$. **H** and **I**, Administration of clathrin-mediated endocytosis inhibitors (chlorpromazine or phenylarsine oxide) for 24 h restored the AE1-329-induced reduction of LOX protein. **J**, Quantification of **H** and **I**. $n=4-6$. **K**, Administration of chlorpromazine for 24 h restored the *m*-3M3FBS (0.5 μmol/L)-induced reduction of LOX protein. **L**, Quantification of **K**. $*P<0.05$, $**P<0.01$, $***P<0.001$. Whole cell lysate was used for LOX detection. AE1-329 was used at 1 μmol/L.

LOX have been extensively studied. Interferon- γ , transforming growth factor- β , platelet-derived growth factor, connective tissue growth factor, and angiotensin II induce LOX gene expression via the interferon regulatory factor 1 transcriptional factor in multiple tissues, including blood vessels.^{40,41} On the other hand, atherogenic concentrations of low-density lipoprotein and tumor necrosis factor α reduce LOX mRNA.^{42,43} Song et al⁴⁴ have also shown that interferon- γ inhibits LOX gene expression through binding to the antagonistic transcriptional factor, interferon regulatory factor 2, in vascular SMCs.

In contrast to our understanding of these transcriptional regulations of LOX, little is known regarding LOX protein metabolism. In the present study, we demonstrated for the first time that the PGE₂-EP4 signal promoted lysosomal degradation of LOX protein. Recently, 1 study that used lysosomal inhibitors and *Vps18*-deficient mice demonstrated that LOX protein was degraded through lysosomes in Purkinje cells.⁴⁵ However, the detailed molecular mechanisms triggering the degradation of LOX protein have not been reported and should be examined in future studies. Once LOX is cleaved from the proenzyme, it acts as a highly reactive enzyme. The mature LOX form catalyzes an oxidative deamination of lysine and hydroxylysine residues to peptidyl α -amino adipic- δ -semialdehydes. These

highly reactive semialdehydes can spontaneously condense to form intra- and intermolecular covalent cross-linkages.²⁷ Elastic fiber formation must be highly regulated to ensure the integrity of vascular and other tissues. Therefore, in addition to transcriptional regulation, the existence of protein regulation of LOX that we demonstrated in this study is physiologically reasonable.

The Rabinovitch group has extensively studied the molecular mechanisms of the sparse elastic fiber formation in the medial layer of the DA. Their studies have demonstrated that LOX activity does not differ between the lamb DA, aorta, and pulmonary artery.⁴⁶ Our study demonstrated that LOX protein was dramatically decreased by EP4 signaling in rodents and humans, suggesting that LOX activity is decreased in these DAs. Currently, we do not have a clear explanation for the apparent inconsistency in terms of LOX expression and activity. Further research is required to determine the species difference in LOX protein metabolism and activity. The Rabinovitch group also demonstrated that there is decreased insolubilization of elastin in the DA that is associated with the truncated 52-kDa tropoelastin that lacks the C terminus,¹² which is unrelated to heightened elastolytic activity.⁴⁶ Similarly, our results showed that matrix metalloproteinase 2

activity does not differ between the DA and the aorta, suggesting that impaired elastogenesis rather than enhanced elastolytic activity provides a muscular arterial property to the DA.

The present study demonstrated that LOX expression is important during development. However, LOX expression is known to be markedly responsive to a variety of pathological states, including wound repair, aging, and tumorigenesis.⁴¹ In particular, strong evidence exists regarding the involvement of a reduction in LOX activity in the pathogenesis of vascular diseases characterized by destructive remodeling of the arterial wall. Previous reports demonstrated that aortic aneurysm and coronary dissections were related to a disturbance in LOX expression in animal models and humans.^{47,48} Therefore, the regulation of LOX expression is considered an attractive therapeutic target. In this study, it should be noted that there seems to be a threshold value for EP4 expression to induce a decrease in elastic fibers and LOX (Figures 2C and 4B). In our previous report, analyses of human aortic aneurysmal tissues demonstrated that EP4 expression is greater in aneurysmal lesions than that in nondiseased areas.⁴⁹ Further studies are required to investigate whether EP4-mediated LOX regulation plays a role in pathological conditions.

Taken together, these findings suggest that PGE₂-EP4 signaling inhibits elastogenesis in the DA by degrading LOX protein. The PGE₂-EP4-mediated LOX protein regulation via a previously unrecognized signaling pathway may also provide the basis for therapeutic strategies that target vascular elastogenesis.

Acknowledgments

We thank Professor S. Narumiya (Department of Pharmacology, Kyoto University Faculty of Medicine, Kyoto, Japan) for kindly providing EP4^{-/-} mice. We thank Professor S. Morita and Dr M. Taguri (Department of Biostatistics and Epidemiology, Yokohama City University, Yokohama, Japan) for assistance with statistical analysis. The adenoviruses of EP4 and LOX were kindly provided from Dr Y. Kobayashi (Matsumoto Dental University, Matsumoto, Japan) and Dr K. Yoshimura (Yamaguchi University, Yamaguchi, Japan), respectively. We also thank Yuka Sawada for histological analyses.

Sources of Funding

This work was supported by grants from the Ministry of Health, Labor, and Welfare of Japan (Y.I.), the Ministry of Education, Culture, Sports, Science, and Technology of Japan (Y.I., U.Y., S.S., M.M., S.M.), a Grant-in-Aid for Scientific Research on Innovative Areas (23116514 and 25116719 to U.Y., 22136009 to Y.I.), the Kitsuen Kagaku Research Foundation (Y.I.), the Foundation for Growth Science (S.M.), the Yokohama Foundation for Advanced Medical Science (U.Y., S.M.), the "High-Tech Research Center" Project for Private Universities: MEXT (S.M.), MEXT-Supported Program for the Strategic Research Foundation at Private Universities (S.M.), the Vehicle Racing Commemorative Foundation (U.Y., S.M.), Miyata Cardiology Research Promotion Funds (U.Y., S.M.), the Takeda Science Foundation (Y.I., U.Y., S.M.), the Japan Heart Foundation Research Grant (U.Y.), the Kowa Life Science Foundation (U.Y.), the Sumitomo Foundation (U.Y.), and the Shimabara Science Promotion Foundation (S.M.).

Disclosures

None.

References

1. Wagenseil JE, Mecham RP. Vascular extracellular matrix and arterial mechanics. *Physiol Rev*. 2009;89:957–989.

2. Wagenseil JE, Ciliberto CH, Knutsen RH, Levy MA, Kovacs A, Mecham RP. The importance of elastin to aortic development in mice. *Am J Physiol Heart Circ Physiol*. 2010;299:H257–H264.
3. Jager BV, Wollenman OJ. An Anatomical Study of the Closure of the Ductus Arteriosus. *Am J Pathol*. 1942;18:595–613.
4. de Reeder EG, van Munsteren CJ, Poelmann RE, Patterson DF, Gittenberger-de Groot AC. Changes in distribution of elastin and elastin receptor during intimal cushion formation in the ductus arteriosus. *Anat Embryol (Berl)*. 1990;182:473–480.
5. Ho SY, Anderson RH. Anatomical closure of the ductus arteriosus: a study in 35 specimens. *J Anat*. 1979;128(pt 4):829–836.
6. Toda T, Tsuda N, Takagi T, Nishimori I, Leszczynski D, Kummerow F. Ultrastructure of developing human ductus arteriosus. *J Anat*. 1980;131(pt 1):25–37.
7. Tada T, Kishimoto H. Ultrastructural and histological studies on closure of the mouse ductus arteriosus. *Acta Anat (Basel)*. 1990;139:326–334.
8. Schaeffer JP. The behavior of elastic tissue in the postfetal occlusion and obliteration of the ductus arteriosus (BOTALLI) in SUS SCROFA. *J Exp Med*. 1914;19:129–142.
9. Jaques A, Serafini-Fracassini A. Morphogenesis of the elastic fiber: an immunoelectronmicroscopy investigation. *J Ultrastruct Res*. 1985;92:201–210.
10. Gittenberger-de Groot AC. Persistent ductus arteriosus: most probably a primary congenital malformation. *Br Heart J*. 1977;39:610–618.
11. Gittenberger-de Groot AC, Moulart AJ, Hitchcock JF. Histology of the persistent ductus arteriosus in cases of congenital rubella. *Circulation*. 1980;62:183–186.
12. Hinek A, Rabinovitch M. The ductus arteriosus migratory smooth muscle cell phenotype processes tropoelastin to a 52-kDa product associated with impaired assembly of elastic laminae. *J Biol Chem*. 1993;268:1405–1413.
13. Hinek A, Mecham RP, Keeley F, Rabinovitch M. Impaired elastin fiber assembly related to reduced 67-kD elastin-binding protein in fetal lamb ductus arteriosus and in cultured aortic smooth muscle cells treated with chondroitin sulfate. *J Clin Invest*. 1991;88:2083–2094.
14. Mitchell MD, Lucas A, Etches PC, Brunt JD, Turnbull AC. Plasma prostaglandin levels during early neonatal life following term and pre-term delivery. *Prostaglandins*. 1978;16:319–326.
15. Woodward DF, Jones RL, Narumiya S. International Union of Basic and Clinical Pharmacology. LXXXIII: classification of prostanoid receptors, updating 15 years of progress. *Pharmacol Rev*. 2011;63:471–538.
16. Yokoyama U, Minamisawa S, Quan H, Ghatak S, Akaike T, Segi-Nishida E, Iwasaki S, Iwamoto M, Misra S, Tamura K, Hori H, Yokota S, Toole BP, Sugimoto Y, Ishikawa Y. Chronic activation of the prostaglandin receptor EP4 promotes hyaluronan-mediated neointimal formation in the ductus arteriosus. *J Clin Invest*. 2006;116:3026–3034.
17. Segi E, Sugimoto Y, Yamasaki A, Aze Y, Oida H, Nishimura T, Murata T, Matsuoka T, Ushikubi F, Hirose M, Tanaka T, Yoshida N, Narumiya S, Ichikawa A. Patent ductus arteriosus and neonatal death in prostaglandin receptor EP4-deficient mice. *Biochem Biophys Res Commun*. 1998;246:7–12.
18. Smith GC, Wu WX, Nijland MJ, Koenen SV, Nathanielsz PW. Effect of gestational age, corticosteroids, and birth on expression of prostanoid EP receptor genes in lamb and baboon ductus arteriosus. *J Cardiovasc Pharmacol*. 2001;37:697–704.
19. Leonhardt A, Glaser A, Wegmann M, Schranz D, Seyberth H, Nüsling R. Expression of prostanoid receptors in human ductus arteriosus. *Br J Pharmacol*. 2003;138:655–659.
20. Rabinovitch M. Cell-extracellular matrix interactions in the ductus arteriosus and perinatal pulmonary circulation. *Semin Perinatol*. 1996;20:531–541.
21. Yokoyama U, Minamisawa S, Ishikawa Y. Regulation of vascular tone and remodeling of the ductus arteriosus. *J Smooth Muscle Res*. 2010;46:77–87.
22. Yokoyama U, Minamisawa S, Quan H, Akaike T, Suzuki S, Jin M, Jiao Q, Watanabe M, Otsu K, Iwasaki S, Nishimaki S, Sato M, Ishikawa Y. Prostaglandin E2-activated Epac promotes neointimal formation of the rat ductus arteriosus by a process distinct from that of cAMP-dependent protein kinase A. *J Biol Chem*. 2008;283:28702–28709.
23. Yokoyama U, Minamisawa S, Katayama A, Tang T, Suzuki S, Iwatsubo K, Iwasaki S, Kurotani R, Okumura S, Sato M, Yokota S, Hammond HK, Ishikawa Y. Differential regulation of vascular tone and remodeling via stimulation of type 2 and type 6 adenylyl cyclases in the ductus arteriosus. *Circ Res*. 2010;106:1882–1892.
24. Hirai M, Ohbayashi T, Horiguchi M, Okawa K, Hagiwara A, Chien KR, Kita T, Nakamura T. Fibulin-5/DANCE has an elastogenic organizer activity that is abrogated by proteolytic cleavage in vivo. *J Cell Biol*. 2007;176:1061–1071.

25. Nguyen M, Camenisch T, Snouwaert JN, Hicks E, Coffman TM, Anderson PA, Malouf NN, Koller BH. The prostaglandin receptor EP4 triggers remodelling of the cardiovascular system at birth. *Nature*. 1997;390:78–81.
26. Nakamura T, Lozano PR, Ikeda Y, Iwanaga Y, Hinek A, Minamisawa S, Cheng CF, Kobuke K, Dalton N, Takada Y, Tashiro K, Ross J Jr, Honjo T, Chien KR. Fibulin-5/DANCE is essential for elastogenesis in vivo. *Nature*. 2002;415:171–175.
27. Rodríguez C, Martínez-González J, Raposo B, Alcudia JF, Guadall A, Badimon L. Regulation of lysyl oxidase in vascular cells: lysyl oxidase as a new player in cardiovascular diseases. *Cardiovasc Res*. 2008;79:7–13.
28. Mäki JM, Räsänen J, Tikkanen H, Sormunen R, Mäkilallio K, Kivirikko KI, Soininen R. Inactivation of the lysyl oxidase gene *Lox* leads to aortic aneurysms, cardiovascular dysfunction, and perinatal death in mice. *Circulation*. 2002;106:2503–2509.
29. Elzenga NJ, Gittenberger-de Groot AC. Localised coarctation of the aorta. An age dependent spectrum. *Br Heart J*. 1983;49:317–323.
30. Jimenez M, Daret D, Choussat A, Bonnet J. Immunohistological and ultrastructural analysis of the intimal thickening in coarctation of human aorta. *Cardiovasc Res*. 1999;41:737–745.
31. Kim JJ, Lakshminathan V, Frilot N, Daaka Y. Prostaglandin E2 promotes lung cancer cell migration via EP4-betaArrestin1-c-Src signaling. *Mol Cancer Res*. 2010;8:569–577.
32. Buchanan FG, Gorden DL, Matta P, Shi Q, Matrisian LM, DuBois RN. Role of beta-arrestin 1 in the metastatic progression of colorectal cancer. *Proc Natl Acad Sci USA*. 2006;103:1492–1497.
33. Wang J, Yin G, Menon P, Pang J, Smolock EM, Yan C, Berk BC. Phosphorylation of G protein-coupled receptor kinase 2-interacting protein 1 tyrosine 392 is required for phospholipase C-gamma activation and podosome formation in vascular smooth muscle cells. *Arterioscler Thromb Vasc Biol*. 2010;30:1976–1982.
34. Mazharian A, Thomas SG, Dhanjal TS, Buckley CD, Watson SP. Critical role of Src-Syk-PLC γ 2 signaling in megakaryocyte migration and thrombopoiesis. *Blood*. 2010;116:793–800.
35. Min C, Kirsch KH, Zhao Y, Jeay S, Palamakumbura AH, Trackman PC, Sonenshein GE. The tumor suppressor activity of the lysyl oxidase propeptide reverses the invasive phenotype of Her-2/neu-driven breast cancer. *Cancer Res*. 2007;67:1105–1112.
36. Regan JW. EP2 and EP4 prostanoid receptor signaling. *Life Sci*. 2003;74:143–153.
37. Ma YC, Huang J, Ali S, Lowry W, Huang XY. Src tyrosine kinase is a novel direct effector of G proteins. *Cell*. 2000;102:635–646.
38. Kagan HM, Li W. Lysyl oxidase: properties, specificity, and biological roles inside and outside of the cell. *J Cell Biochem*. 2003;88:660–672.
39. Mäki JM, Sormunen R, Lippo S, Kaartenaho-Wiik R, Soininen R, Myllyharju J. Lysyl oxidase is essential for normal development and function of the respiratory system and for the integrity of elastic and collagen fibers in various tissues. *Am J Pathol*. 2005;167:927–936.
40. Yoshimura K, Aoki H, Ikeda Y, Fujii K, Akiyama N, Furutani A, Hoshii Y, Tanaka N, Ricci R, Ishihara T, Esato K, Hamano K, Matsuzaki M. Regression of abdominal aortic aneurysm by inhibition of c-Jun N-terminal kinase. *Nat Med*. 2005;11:1330–1338.
41. Smith-Mungo LI, Kagan HM. Lysyl oxidase: properties, regulation and multiple functions in biology. *Matrix Biol*. 1998;16:387–398.
42. Rodríguez C, Alcudia JF, Martínez-González J, Raposo B, Navarro MA, Badimon L. Lysyl oxidase (LOX) down-regulation by TNFalpha: a new mechanism underlying TNFalpha-induced endothelial dysfunction. *Atherosclerosis*. 2008;196:558–564.
43. Rodríguez C, Raposo B, Martínez-González J, Casanf L, Badimon L. Low density lipoproteins downregulate lysyl oxidase in vascular endothelial cells and the arterial wall. *Arterioscler Thromb Vasc Biol*. 2002;22:1409–1414.
44. Song YL, Ford JW, Gordon D, Shanley CJ. Regulation of lysyl oxidase by interferon-gamma in rat aortic smooth muscle cells. *Arterioscler Thromb Vasc Biol*. 2000;20:982–988.
45. Peng C, Yan S, Ye J, Shen L, Xu T, Tao W. Vps18 deficiency inhibits dendritogenesis in Purkinje cells by blocking the lysosomal degradation of Lysyl Oxidase. *Biochem Biophys Res Commun*. 2012;423:715–720.
46. Zhu L, Dagher E, Johnson DJ, Bedell-Hogan D, Keeley FW, Kagan HM, Rabinovitch M. A developmentally regulated program restricting insolubilization of elastin and formation of laminae in the fetal lamb ductus arteriosus. *Lab Invest*. 1993;68:321–331.
47. Nakashima Y, Sueishi K. Alteration of elastic architecture in the lathyrus rat aorta implies the pathogenesis of aortic dissecting aneurysm. *Am J Pathol*. 1992;140:959–969.
48. Sibon I, Sommer P, Lamaziere JM, Bonnet J. Lysyl oxidase deficiency: a new cause of human arterial dissection. *Heart*. 2005;91:e33.
49. Yokoyama U, Ishiwata R, Jin MH, Kato Y, Suzuki O, Jin H, Ichikawa Y, Kumagaya S, Katayama Y, Fujita T, Okumura S, Sato M, Sugimoto Y, Aoki H, Suzuki S, Masuda M, Minamisawa S, Ishikawa Y. Inhibition of EP4 signaling attenuates aortic aneurysm formation. *PLoS ONE*. 2012;7:e36724.

CLINICAL PERSPECTIVE

The ductus arteriosus (DA) is a fetal bypass artery between the aorta and the pulmonary artery. Although the DA closes immediately after birth, it remains open in some infants, a condition known as patent DA. Patent DA remains a frequent problem among premature infants with significant morbidity and mortality. Both vascular contraction and remodeling (ie, intimal thickening) are required for complete anatomical closure of the DA. Decreased elastogenesis is known as a hallmark of DA remodeling and is thought to contribute to intimal thickening of the DA. However, the molecular mechanisms of decreased elastogenesis are not fully understood. Herein, we show that prostaglandin E₂ (PGE₂) receptor EP4 signaling promotes degradation of the mature lysyl oxidase protein, a cross-linking enzyme for elastic fibers, only in the DA, leading to decreased elastogenesis. The newly recognized PGE-EP4-c-Src-PLC γ -signaling pathway most likely contributes to the lysosomal degradation of lysyl oxidase. Based on these data, it appears that PGE-EP4 signaling is required for DA remodeling and that inhibition of this signaling by cyclooxygenase inhibitors may attenuate DA remodeling after birth, especially in premature infants in which the DA is not fully remodeled. Activation of the c-Src-PLC γ signaling pathway may be an additional strategy to promote anatomical closure of the immature DA.

SUPPLEMENTAL MATERIAL

Supplemental Methods

Reagents

8-p-Methoxyphenylthio-2-Omethyl-cAMP (pMe-cAMP) and N6-benzoyladenosine-cAMP (Bnz-cAMP) were purchased from BioLog Life Science Institute (Bremen, Germany) and Sigma (St. Louis, MO), respectively. PGE₂, sulprostone, butaprost, gallein, BAPN, bisindolylmaleimide (bis), U73122, U0126, LY294002, PAO, EIPA, and 8-Bromo-cAMP (Br-cAMP) were purchased from Sigma-Aldrich (St. Louis, MO). CPZ, MβCD, MG132, and NH₄Cl were obtained from Wako (Osaka, Japan). The PKA inhibitor (14–22), bafilomycin A1, PP2, and m-3M3FBS were obtained from Calbiochem (Darmstadt, Germany). ONO-AE1-329 was kindly provided by ONO Pharmaceutical Company (Osaka, Japan). Antibodies for LOX and pro-LOX for immunoblotting were obtained from Abcam (Cambridge, UK) and Novus Biological (Littleton, CO), respectively. Anti-LOX antibody for immunohistochemistry and anti-BMP-1 were obtained from US Biological (Swampscott, MA) and Santa Cruz Biotechnology (Santa Cruz, CA), respectively. Anti-elastin and anti-EP4 antibodies were obtained from Elastin Products Company (Owensville, MO) and Caymanchemical (Ann Arbor, MI), respectively. Anti-PLCγ and anti-phosphorylated PLCγ antibodies were obtained from Cell Signaling (Beverly, MA). Anti-MMP-2 and anti-MMP-9 antibodies were from R&D Systems (Minneapolis, MN). Anti-fibrillin-1 antibody was kindly

provided from Dr. Nakamura (Kansai University, Japan).

Isolation and culture of rat smooth muscle cells (SMCs)

Vascular SMCs were obtained from the DA and aorta of Wistar rat fetuses on the 21st day of gestation (SLC Inc.) as previously described¹. Using the same protocol, pulmonary SMCs were isolated from the branch extralobular pulmonary arteries from Wistar rats on the 21st day of gestation. SMCs were used at passages 4 to 6.

Immunoblot analysis

Proteins from whole cells were analyzed by immunoblotting as previously described¹.

Adenovirus construction

Adenovirus of EP4 was kindly provided from Dr. Y. Kobayashi (Matsumoto Dental University, Japan)². A control adenovirus vector with LacZ was used at the same multiplicity of infection.

RNA interference (siRNA)

Double-stranded siRNAs to the selected regions of EP4 (stealth RNAi RSS331316) and the negative siRNA purchased from Invitrogen (San Diego, CA). According to the manufacturer's instructions, cells were transfected with siRNA (300 pmol), using Lipofectamin RNAiMAX (Invitrogen).

Quantitative and semi-quantitative reverse transcriptase-polymerase chain reaction

(RT-PCR)

Isolation of total RNA and generation of cDNA were performed and RT-PCR analysis was done

as previously described ¹. The primers were designed based on the rat nucleotide sequences of EP4 (5'-CTC GTG GTG CGA GTG TTC AT-3' and 5'-AAG CAA TTC TGA TGG CCT GC-3') and BMP-1 (5'-CAT CTC CAT CGG CAA GAA C-3' and 5'-CTC GAC TTC CTG AAC TTC CAT C-3'). Each primer set was designed between multiple exons. The abundance of each gene was determined relative to the 18S transcript.

Electron microscopy

Electron microscopic analysis for elastic fiber formation was performed as previously described ³.

Gelatin zymography

MMP activity was examined by gelatin zymography as previously described ⁴.

In situ hybridization

Expression of EP4 mRNA in mice fetuses on day 12.5, 16.5, and 18.5 of gestation was evaluated by *in situ* hybridization. A 543 bp DNA fragment corresponding to nucleotide positions 1373 to 1915 of mouse EP4 cDNA (Gen-Bank NM_008965) was cloned into pGEMT-Easy vector (Promega, Madison, WI) and used for the generation of sense and antisense RNA probes. Digoxigenin-labeled RNA probes were prepared with DIG RNA Labeling Mix (Roche, Basel, Switzerland). Hybridization was performed with probes at concentrations of 300 ng/ml in the Probe Diluent-1 (Genostaff, Tokyo, Japan) at 60°C for 16 h. After treatment with 0.5% blocking reagent (Roche) in TBST for 30 min, the sections were incubated with anti-DIG AP conjugate (Roche) diluted 1:1000 with TBST for 2 hr at room temperature (RT). Coloring reactions were

performed with NBT/BCIP solution overnight and then washed with PBS. The sections were counterstained with Kernechtrot stain solution (Muto Pure Chemicals, Tokyo, Japan), and mounted with CC/Mount (DBS).

Supplemental Table 1.

Summary of patient profile

Case	Age at Operation	Diagnosis
1	2 days	CoA, VSD
2	3 days	TGA, CoA
3	4 days	CoA, VSD
4	4 days	CoA, VSD
5	13 days	CoA, VSD
6	13 days	CoA, VSD
7	1 month	hypoLV, CoA, VSD

CoA: Coarctation of the Aorta, VSD: Ventricular Septum Defect,

TGA: Transposition of the Great Arteries, hypoLV: hypoplastic Left
Ventricle.

Supplemental table 2.

Correlation between elastic fiber formation and expression of EP4 and LOX

case	Elastic fiber formation - EP4			Elastic fiber formation - LOX			EP4 - LOX		
	r	n	p value	r	n	p value	r	n	p value
1	-0.7164	68	< 0.0001***	0.8095	68	< 0.0001***	-0.6723	68	< 0.0001***
2	-0.8277	22	< 0.0001***	0.6043	22	0.0029**	-0.6101	22	0.0026**
3	-0.8869	44	< 0.0001***	0.6431	44	< 0.0001***	-0.5626	44	< 0.0001***
4	-0.7116	62	< 0.0001***	0.765	62	< 0.0001***	-0.4875	62	< 0.0001***
5	-0.547	35	0.0007***	0.7561	35	< 0.0001***	-0.5335	35	0.001***
6	-0.523	28	0.0043**	0.6032	28	0.0007***	-0.6066	28	0.0006***
7	-0.7851	19	< 0.0001***	0.8649	19	< 0.0001***	-0.5765	19	0.0098**

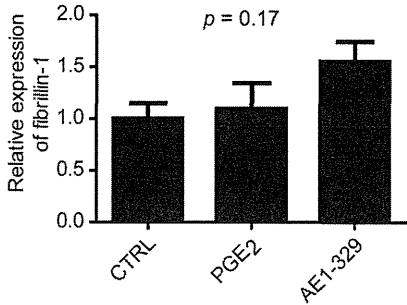
r: correlation coefficient; n: number of sampling points. *, $p < 0.05$; **, $p < 0.01$; ***, $p < 0.001$

Supplemental Figure 1

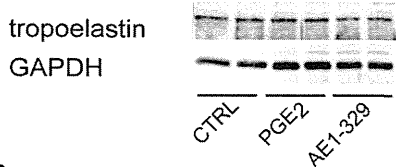
A



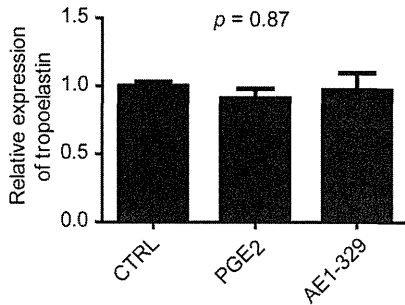
B



C

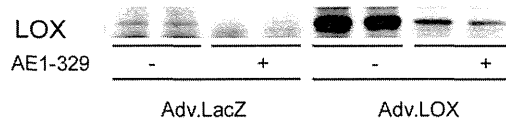


D

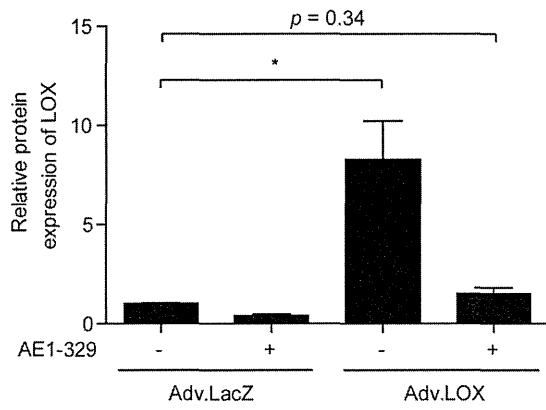


Supplemental Figure 2

A

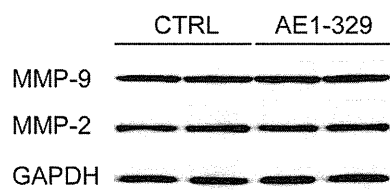


B

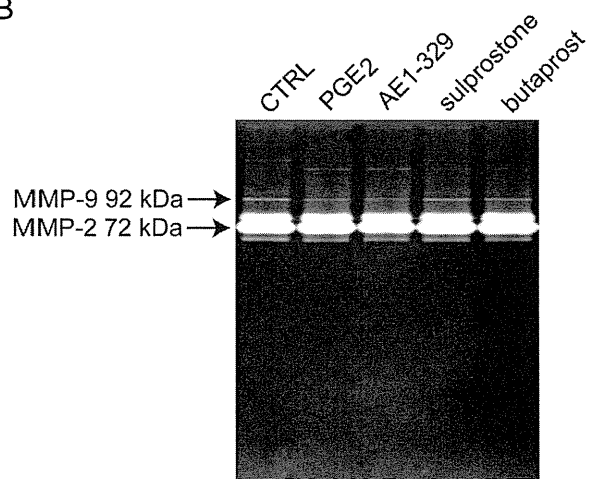


Supplemental Figure 3

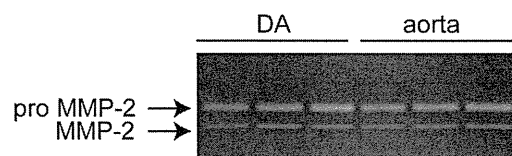
A



B

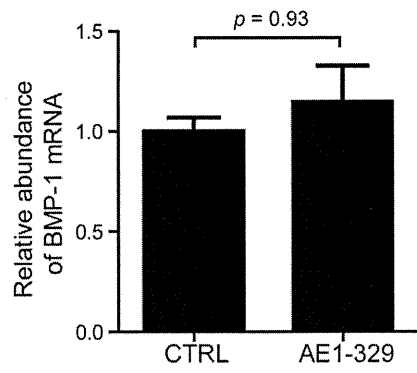


C

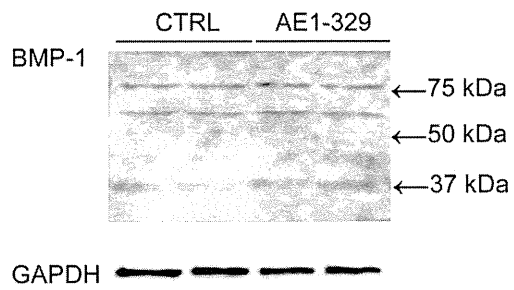


Supplemental Figure 4

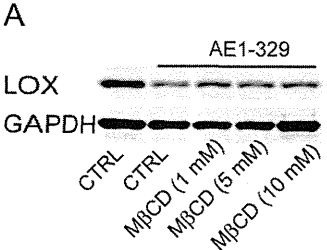
A



B



Supplemental Figure 5



Supplemental Figure Legends

Supplemental Figure 1

EP4 signaling did not affect protein expression of tropoelastin and fibrillin-1.

(A) Protein expression of fibrillin-1 in culture medium of DASCs treated with either PBS, PGE₂ (1 μM), or AE-329 (1 μM) for 72 h. (B) Quantification of (A), n = 4. (C) Protein expression of tropoelastin in whole cell lysate of DASCs treated with either PBS, PGE₂ (1 μM), or AE-329 (1 μM) for 72 h. (D) Quantification of (C), n = 4.

Supplemental Figure 2

Overexpression of LOX protein in DASCs transfected with Adv.LOX.

(A) Protein expression of LOX in culture medium of DASCs transfected Adv.LacZ or Adv.LOX in the presence or absence of AE-329 (1 μM). The time-course of transfection and drug administration was same as Figure 4I. (B) Quantification of (A), n = 4, **p* < 0.05.

Supplemental Figure 3

EP4 signaling did not affect expression or activation of MMP-2 or -9 in DASCs.

(A) Protein expression of MMP-2 and-9 in DASCs treated with or without AE1-329 (1 μM) for 72 h. (B) Gelatin zymography of DASCs treated with 1 μM of PGE₂ or each EP agonist. (C) Gelatin zymography of the rat DA and aorta on the 21st day of gestation.

Supplemental Figure 4

EP4 signaling did not change BMP-1 expression in DASCs.

(A) Expression of BMP-1 mRNA in DASCs treated with or without AE1-329 (1 μ M) for 24 h.

n = 4. (B) Representative image of protein expression of BMP-1 in DASCs treated with or without AE1-329 (1 μ M) for 72 h.

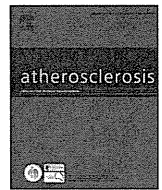
Supplemental Figure 5

LOX degradation was associated with caveolar endocytosis, macropinocytosis, and proteasome.

(A) Representative figures of protein expression of LOX in whole cell lysate of DASCs treated with MbCD, EIPA, or MG132 in the presence of AE1-329 (1 μ M).

References

1. Yokoyama U, Minamisawa S, Adachi-Akahane S, Akaike T, Naguro I, Funakoshi K, Iwamoto M, Nakagome M, Uemura N, Hori H, Yokota S, Ishikawa Y. Multiple transcripts of ca^{2+} channel $\alpha 1$ -subunits and a novel spliced variant of the $\alpha 1c$ -subunit in rat ductus arteriosus. *Am J Physiol Heart Circ Physiol*. 2006;290:H1660-1670
2. Kobayashi Y, Take I, Yamashita T, Mizoguchi T, Ninomiya T, Hattori T, Kurihara S, Ozawa H, Udagawa N, Takahashi N. Prostaglandin e_2 receptors ep_2 and ep_4 are down-regulated during differentiation of mouse osteoclasts from their precursors. *J Biol Chem*. 2005;280:24035-24042
3. Nakamura T, Lozano PR, Ikeda Y, Iwanaga Y, Hinek A, Minamisawa S, Cheng CF, Kobuke K, Dalton N, Takada Y, Tashiro K, Ross Jr J, Honjo T, Chien KR. Fibulin-5/dance is essential for elastogenesis in vivo. *Nature*. 2002;415:171-175
4. Yoshimura K, Aoki H, Ikeda Y, Fujii K, Akiyama N, Furutani A, Hoshii Y, Tanaka N, Ricci R, Ishihara T, Esato K, Hamano K, Matsuzaki M. Regression of abdominal aortic aneurysm by inhibition of c-jun n-terminal kinase. *Nat Med*. 2005;11:1330-1338



Three-dimensional multilayers of smooth muscle cells as a new experimental model for vascular elastic fiber formation studies



Ryo Ishiwata^a, Utako Yokoyama^{a,*}, Michiya Matsusaki^b, Yoshiya Asano^c, Koji Kadowaki^b, Yasuhiro Ichikawa^a, Masanari Umemura^a, Takayuki Fujita^a, Susumu Minamisawa^d, Hiroshi Shimoda^c, Mitsuru Akashi^b, Yoshihiro Ishikawa^{a,*}

^a Cardiovascular Research Institute, Yokohama City University Graduate School of Medicine, 3-9 Fukuura, Kanazawa-ku, Yokohama, Kanagawa 236-0004, Japan

^b Department of Applied Chemistry, Graduate School of Engineering, Osaka University, Osaka, Japan

^c Department of Neuroanatomy, Cell Biology and Histology, Hirosaki University Graduate School of Medicine, Hirosaki, Japan

^d Department of Cell Physiology, Jikei University School of Medicine, Tokyo, Japan

ARTICLE INFO

Article history:

Received 9 August 2013

Received in revised form

20 January 2014

Accepted 21 January 2014

Available online 29 January 2014

Keywords:

Blood vessels
Smooth muscle cells
Elastic fibers
Nanotechnology
Tissue engineering
Fibronectin

ABSTRACT

Objective: Elastic fiber formation is disrupted with age and by health conditions including aneurysms and atherosclerosis. Despite considerable progress in the understanding of elastogenesis using the planar culture system and genetically modified animals, it remains difficult to restore elastic fibers in diseased vessels. To further study the molecular mechanisms, in vitro three-dimensional vascular constructs need to be established. We previously fabricated vascular smooth muscle cells (SMCs) into three-dimensional cellular multilayers (3DCMs) using a hierarchical cell manipulation technique, in which cells were coated with fibronectin-gelatin nanofilms to provide adhesive nano-scaffolds. Since fibronectin is known to assemble and activate elastic fiber-related molecules, we further optimized culture conditions.

Methods and results: Elastica stain, immunofluorescence, and electron microscopic analysis demonstrated that 3DCMs, which consisted of seven layers of neonatal rat aortic SMCs cultured in 1% fetal bovine serum (FBS) in Dulbecco's modified Eagle's medium, exhibited layered elastic fibers within seven days of being in a static culture condition. In contrast, the application of adult SMCs, 10% FBS, *e*-poly(-lysine) as an alternative adhesive for fibronectin, or four-layered SMCs, failed to generate layered elastic fiber formation. Radioimmunoassay using [³H]valine further confirmed the greater amount of cross-linked elastic fibers in 3DCMs than in monolayered SMCs. Layered elastic fiber formation in 3DCMs was inhibited by the lysyl oxidase inhibitor β -aminopropionitrile, or prostaglandin E₂. Furthermore, infiltration of THP-1-derived macrophages decreased the surrounding elastic fiber formation in 3DCMs. **Conclusion:** 3DCMs may offer a new experimental vascular model to explore pharmacological therapeutic strategies for disordered elastic fiber homeostasis.

© 2014 Elsevier Ireland Ltd. All rights reserved.

1. Introduction

Arterial walls have a highly organized layer structure that consists of various cells and extracellular matrix (ECM) components. In particular, the vascular media is composed of a dense population of concentrically organized smooth muscle cells (SMCs) and elastic fibers, and plays a pivotal role in maintaining sufficient blood

pressure, even during variations in hemodynamic stress. In physiological conditions, SMCs synthesize elastin and other specific molecules, which are incorporated into elastic fibers and arranged into concentric rings of elastic lamellae around the arterial media [1]. In contrast, arterial compliance and distensibility are impaired in the presence of cardiovascular disease and risk factors such as aortic aneurysm, atherosclerosis, ischemic heart disease, aging, hypertension, cigarette smoking, and diabetes [2]. Hence, impaired elastic properties are associated with arterial dysfunction and pathophysiology [2,3].

Changes in arterial elastic properties are the result of alterations in the intrinsic structural properties of the artery, including the fracturing and thinning of elastic fibers. Current approaches to

* Corresponding authors. Tel.: +81 45 787 2575; fax: +81 45 787 1470.

E-mail addresses: utako@yokohama-cu.ac.jp, CZL03430@nifty.com (U. Yokoyama), yishikaw@med.yokohama-cu.ac.jp (Y. Ishikawa).

examining the elastogenesis and degradation of elastic fibers rely heavily on the use of the planar culture of vascular SMCs and genetically modified animals. These approaches have been instrumental in numerous discoveries and have been modified to create very elegant experimental designs [1,4–7]. Currently, however, no pharmacological strategy to promote elastogenesis and prevent the degradation of elastic fiber formation is available, and the molecular mechanisms of the regulation of elastic fiber formation remain to be studied. The two-dimensional (2D) monolayer culture system is a useful method for isolating specific factors and their effects on specific cell types [5–7], but it lacks the native-like layered structure of elastic fibers. Therefore, changes in the spatial arrangement of elastic fibers induced by various stimuli and the infiltration of immune cells cannot be observed. In-vivo analysis, on the other hand, often fails to discriminate among the various and complex factors. In this context, in vitro reconstruction vessel models overcoming these limitations are considered potential platforms of vascular biology that can provide further insights into the spatio-temporal molecular mechanisms of elastic fiber formation.

We previously developed a novel three-dimensional (3D) cell construction method [8] and created 3D-layered blood vessel constructs consisting of human umbilical arterial SMCs and human umbilical vascular endothelial cells [9]. To develop the 3D-cellular multilayers (3DCMs), we fabricated nanometer-sized cell adhesives like ECM scaffolds onto the surface of a cell membrane, which enables another cellular layer to adhere to the coated cell surface. We employed a layer-by-layer (LbL) technique to fabricate fibronectin–gelatin nanofilms onto living cell membranes, because the LbL technique produces nanometer-sized polymer films with a controllable nanometer thickness through the alternate immersion into interactive polymer solutions. We found that approximately 6 nm of fibronectin-based nanofilms were suitable for developing stable adhesive scaffolds and for creating allogeneic or xenogeneic multiple cell layers.

In addition to the cell adhesion effect, fibronectin has been known to orchestrate the assembly of the ECM [10–15]. In particular, recent reports suggest that fibronectin fiber assembles pericellularly into fibrillin microfibrils that have a complex structural organization and are widespread in elastic tissues [10,16]. Furthermore, fibronectin binds to lysyl oxidase (LOX), a cross-linking enzyme for elastic fibers, and acts as a scaffold for enzymatically active 30 kDa LOX [14]. Using scanning electron microscopy and transmission electron microscopy, we observed that fibronectin formed extracellular fibrils in the abovementioned 3DCMs within 24 h cultures [9], suggesting that fibronectin-coated SMCs have the potential to produce elastic fiber assemblies. In this context, we aimed to create the first scaffold-free 3D cellular multilayers (3DCMs) that are specifically designed for investigating the spatial regulation of vascular elastic fibers by employing this LbL assembly technique. The present study demonstrates that the optimized culture conditions provided layered elastic fiber formation in the 3DCMs consisting of neonatal rat SMCs within seven days of static culture conditions. In the 3DCMs, it was observed in the vertical view that macrophage infiltration or prostaglandin E₂ (PGE₂) changed the spatial arrangement of elastic fibers.

2. Materials and methods

Expanded materials and methods are described in Supplemental data.

2.1. Animals

Neonate (day 1) and adult Wistar rats (4–5months old) were obtained from Japan SLC, Inc. (Shizuoka, Japan). All animal studies

were approved by the institutional animal care and use committees of Yokohama City University.

2.2. Cell culture

Vascular SMCs in primary culture were obtained from the aorta of rat neonates (day 1) as previously described [17–19]. Briefly, the minced tissues were digested with a collagenase-dispase enzyme mixture at 37 °C for 20 min. The cell suspensions were then centrifuged, and the medium was changed to a collagenase II enzyme mixture. After 12 min of incubation at 37 °C, cell suspensions were plated on 35 mm poly-L-lysine-coated dishes. The growth medium contained Dulbecco's modified Eagle medium (DMEM) with 10% fetal bovine serum (FBS), 100 U/ml penicillin, and 100 mg/ml streptomycin (Invitrogen, Carlsbad, CA). Human adult aortic SMCs were obtained from Lonza (Walkersville, MD, USA). The confluent SMCs were used at passages 5–7. THP-1 cells were obtained from the Health Science Research Resources Bank (Osaka, Japan) and were maintained in RPMI 1640 medium (Wako, Osaka, Japan) supplemented with 10% FBS. All cells were cultured in a moist tissue culture incubator at 37 °C in 5% CO₂–95% ambient mixed air.

2.3. Construction of 3DCMs

Construction of 3DCMs was performed as previously described [8]. Briefly, a cell disk LF (Sumitomo Bakelite, Tochigi, Japan) was rinsed with 50 mM Tris–HCl buffer solution (pH 7.4) for 15 min and coated with fibronectin (0.2 mg/ml) for 30 min at 37 °C. SMCs were cultured on the cell disk (11×10^4 cells/cm²) and incubated for 12 h in 10% FBS/DMEM. The monolayered SMCs were then immersed alternatively in a solution of fibronectin (0.2 mg/ml) and gelatin (0.2 mg/ml). After nine steps of LbL assembly with fibronectin and gelatin, a second cell layer was seeded on the first cell layer (11×10^4 cells/cm²) and incubated for 6–12 h at 37 °C. The cycles of LbL nanofilm assembly and subsequent cell seeding were repeated six times in four days to construct seven-layered 3DCMs. During the first four days, the medium was refreshed daily. Twelve hours after the seeding of the last layer, the culture media was changed to DMEM or DMEM/F-12 (Gibco, Carlsbad, CA) containing 1% FBS or 10% FBS. The 3DCMs were incubated for an additional 48 h and either fixed in buffered 10% formalin or harvested in TRIzol (Invitrogen, Carlsbad, CA). The time-course of the 3DCM experiments is shown in Supplemental Fig. 1A. Stimulation by β -aminopropionitrile (BAPN) or PGE₂ (1 μ M) was performed simultaneously with the medium change on day 5. For macrophage infiltration assay, seven-layered 3DCMs at day 5 were put on a 24-well plate and applied with 500 μ l of RPMI 1640 medium containing THP-1 cells (2.0×10^5 cells) with or without phorbol 12-myristate 13-acetate (PMA, 0.1 μ M). The 3DCMs were incubated for 1 h at 37 °C. Next, unattached THP-1 cells were washed out with PBS and 3DCMs were incubated in 1% FBS/DMEM for 72 h until fixation. Control monolayered neonatal rat aortic SMCs (2D-SMCs) were plated on day 4 in the same density as a single layer in 3DCMs (11×10^4 cells/cm²), and were incubated for 48 h. Four-layered 3DCMs were constructed from day 3 following the same time-course. The proportional increase in the thickness of 3DCMs with the number of seeding events was shown in Supplemental Fig. 1B. To confirm the effect of fibronectin nanofilms, ϵ -poly(lysine) (0.2 mg/ml) was used as an alternative adhesive polymer.

2.4. Quantitative measurement of insoluble elastin

Newly synthesized insoluble elastin was measured as previously described [20,21]. Briefly, after the seven-layered 3DCMs and 2D-